

Modifications and Clarifications for the Implementation of the Spalart-Allmaras Turbulence Model

Steven R. Allmaras, Forrester T. Johnson* and Philippe R. Spalart**
corresponding author: steven.r.allmaras@gmail.com

* YourEncore; Boeing Commercial Airplanes retired

** Senior Technical Fellow, Boeing Commercial Airplanes

Abstract: We present modifications to the Spalart-Allmaras (S-A) turbulence model targeted toward situations of under-resolved grids and unphysical transient states. These modifications are formulated to be passive to the original model in well resolved flowfields and should produce negligible differences in most cases. They are motivated primarily by numerical issues near the interface between turbulent and irrotational regions. We also comment on the appropriate form of S-A for compressible flows, the inclusion of the laminar suppression term for fully turbulent flows, and the use of maximum value limiters on the turbulence solution. We also present a new analytic solution to S-A for law of the wall velocity.

Keywords: Computational Fluid Dynamics, Turbulence Modeling.

1 Introduction

The Spalart-Allmaras (S-A) turbulence model [1, 2] has been widely used and has proven to be numerically well behaved in most cases. There are, however, situations of under-resolved grids and unphysical transients where discretization of the model can lead to undesired results. Undershoots at the edge of boundary layers and wakes is one such situation. Another is when the modified vorticity \tilde{S} becomes negative. We propose modifications to the S-A model to remedy these situations. The first is a continuation of S-A for negative $\tilde{\nu}$ solution values that should be applicable to a wide range of discretization methods. The second is a change in the definition of \tilde{S} that avoids negative values, while preserving the original behavior in regions where the correlation is physically relevant.

Many applications of S-A target fully turbulent flows, where the flow is essentially turbulent everywhere vorticity is present. For these flows, inclusion of the laminar suppression term (f_{t2}) is effectively optional since it has negligible effect on the resulting flow. This is the case as long the freestream level of $\tilde{\nu}$ is high enough (e.g. $\tilde{\nu}/\nu = 3-5$). We comment on the appropriate values of freestream $\tilde{\nu}$ in the presence of the f_{t2} term, reiterating the findings of Rumsey and Spalart [3]. We also comment on the misuse of limits on the maximum value attained by the turbulence solution.

The original S-A references formulated a single partial differential equation (PDE) applicable to both incompressible and compressible flows. Unfortunately, there is confusion in the literature on the compressible form of S-A. We clarify the standard form of S-A for compressible flows and comment on associated jump conditions.

We propose a change in the boundary condition imposed on inviscid or slip walls. This is the result of re-examination of blocking effects of the wall on Reynolds stresses.

S-A is formulated to admit simple solutions for $\tilde{\nu}$ and the modified vorticity \tilde{S} for the law of the wall. We present a new analytic solution for the velocity that satisfies S-A in the law of the wall. This solution could be used for wall functions and for code validation.

The paper is organized as follows: In Section 2, the baseline S-A model is restated, followed by discussion of the appropriate compressible form of S-A. Included in this section are comments on the inclusion of the f_{t2} term and appropriate freestream values, as well as comments on the use of limiting maximum values. Then new modifications for S-A are presented in Section 3. These include the redefinition of modified vorticity \tilde{S} , introduction of a negative continuation of S-A, and a proposed change in boundary conditions on $\tilde{\nu}$ for inviscid walls. We emphasize that the modified vorticity redefinition and negative model should have negligible effects on physically relevant, grid-resolved solutions. Finally, in Section 4, we present the new analytic solution for velocity in the law of the wall.

2 Baseline Clarifications

2.1 S-A

For reference we present the baseline S-A model, version Ia of Ref. [2]. Reynolds stresses are evaluated using the Boussinesq eddy viscosity assumption, where the eddy viscosity ν_t is given by

$$\nu_t = \tilde{\nu} f_{v1}, \quad f_{v1} = \frac{\chi^3}{\chi^3 + c_{v1}^3}, \quad \chi \equiv \frac{\tilde{\nu}}{\nu}, \quad (1)$$

where ν is the kinematic viscosity. $\tilde{\nu}$ is the S-A working variable and obeys the transport equation,

$$\frac{D\tilde{\nu}}{Dt} = P - D + T + \frac{1}{\sigma} \left[\nabla \cdot ((\nu + \tilde{\nu})\nabla\tilde{\nu}) + c_{b2} (\nabla\tilde{\nu})^2 \right], \quad (2)$$

where production, wall destruction and trip terms are

$$P = c_{b1}(1 - f_{t2})\tilde{S}\tilde{\nu}, \quad D = \left(c_{w1}f_w - \frac{c_{b1}}{\kappa^2}f_{t2} \right) \left[\frac{\tilde{\nu}}{d} \right]^2, \quad T = f_{t1}(\Delta u)^2 \quad (3)$$

Here \tilde{S} is the modified vorticity,

$$\tilde{S} \equiv S + \frac{\tilde{\nu}}{\kappa^2 d^2} f_{v2}, \quad f_{v2} = 1 - \frac{\chi}{1 + \chi f_{v1}}, \quad (4)$$

where S is the magnitude of the vorticity, and d is the distance to the closest wall. The function f_w is

$$f_w = g \left[\frac{1 + c_{w3}^6}{g^6 + c_{w3}^6} \right]^{1/6}, \quad g = r + c_{w2} (r^6 - r), \quad r = \min \left(\frac{\tilde{\nu}}{\tilde{S}\kappa^2 d^2}, r_{\text{lim}} \right). \quad (5)$$

Trip and laminar suppression terms are

$$f_{t1} = c_{t1}g_t \exp \left(-c_{t2} \frac{\omega_t}{\Delta u^2} [d^2 + g_t^2 d_t^2] \right), \quad f_{t2} = c_{t3} \exp(-c_{t4} \chi^2), \quad (6)$$

with $g_t = \min(0.1, \Delta u/\omega_t \Delta x)$, where d_t is distance to the trip point, ω_t is the vorticity at the trip, Δu is the difference in velocity relative the trip point, and Δx is streamwise grid spacing at the trip. The constants are $c_{b1} = 0.1355$, $\sigma = 2/3$, $c_{b2} = 0.622$, $\kappa = 0.41$, $c_{w1} = c_{b1}/\kappa^2 + (1 + c_{b2})/\sigma$, $c_{w2} = 0.3$, $c_{w3} = 2$, $c_{v1} = 7.1$, $c_{t1} = 1$, $c_{t2} = 2$, $c_{t3} = 1.2$, $c_{t4} = 0.5$, and $r_{\text{lim}} = 10$. Turbulent heat transfer obeys a turbulent Prandtl number equal to 0.9. Boundary conditions for $\tilde{\nu}$ are

$$\text{no-slip wall: } \tilde{\nu} = 0 \quad \text{symmetry plane: } \frac{\partial \tilde{\nu}}{\partial n} = 0 \quad (7)$$

$$\text{freestream (fully turbulent): } \tilde{\nu}/\nu = 3\text{--}5 \quad (\nu_t/\nu \approx 0.2\text{--}1.3) \quad \text{freestream (tripped): } \tilde{\nu}/\nu \ll 1 \quad (8)$$

S-A is documented with various modifications in the excellent NASA Langley Turbulence Modeling Resource website [4].

2.2 Compressible Form of S-A

Confusion exists in the literature over the formulation of S-A for compressible flows. We reaffirm that the formulation presented above is applicable to both incompressible and compressible flows, and it should be considered the standard form for compressible. An equivalent conservation form can be constructed by combining S-A with the mass conservation equation,

$$0 = \rho * \{\text{S-A}\} + \tilde{\nu} * \{\text{mass}\} \\ = \frac{\partial \rho \tilde{\nu}}{\partial t} + \nabla \cdot (\rho \tilde{u} \tilde{\nu}) - \rho(P - D + T) - \frac{1}{\sigma} \nabla \cdot [\rho(\nu + \tilde{\nu}) \nabla \tilde{\nu}] - \frac{c_{b2}}{\sigma} \rho (\nabla \tilde{\nu})^2 + \frac{1}{\sigma} (\nu + \tilde{\nu}) \nabla \rho \cdot \nabla \tilde{\nu} \quad (9)$$

where ρ is density and \tilde{u} is velocity. Molecular viscosity, $\mu = \nu/\rho$, is a function of temperature.

In the absence of vorticity (production) and wall terms, the jump of $\tilde{\nu}$ through shocks is zero. Consider the canonical case of a shock layer separating two constant states. With zero oncoming vorticity, production is zero. Assuming the shock layer is sufficiently far from the nearest wall, then destruction is also zero. Integrating Eq. 9 across the shock layer and imposing Rankine-Hugoniot, the jump in $\tilde{\nu}$ is given by

$$\rho u [[\tilde{\nu}]] = \int_1^2 \left[\frac{c_{b2}}{\sigma} \rho \left(\frac{\partial \tilde{\nu}}{\partial x} \right)^2 - \frac{1}{\sigma} (\nu + \tilde{\nu}) \frac{\partial \rho}{\partial x} \frac{\partial \tilde{\nu}}{\partial x} \right] dx \quad (10)$$

where x is normal to the shock layer and u is the velocity normal to the shock. The zero jump solution follows from the observation that both integrands depend on the gradient of $\tilde{\nu}$; the integral is zero if the gradient is zero throughout the shock layer. Simulations of 1-D shock layers confirm this behavior even across layers of finite thickness produced by moderate upstream values of ν and $\tilde{\nu}$.

We note that while $\tilde{\nu}$ has zero jump, the eddy viscosity ν_t will have nonzero jump. This results from the fact that kinematic viscosity has nonzero jump due to its dependence on temperature and density, both of which have nonzero jumps. The jump in ν feeds into eddy viscosity through the f_{v1} correlation.

2.3 Inclusion of f_{t2} and Appropriate Freestream Values of $\tilde{\nu}$

The f_{t2} laminar suppression term was included in the model to prevent spurious growth of small $\tilde{\nu}$ in the presence of vorticity. Its primary purpose is to prevent premature transition in laminar boundary layers upstream of trips (the f_{t1} term). For fully turbulent flows with adequately large freestream $\tilde{\nu}$ values (e.g. $\tilde{\nu}/\nu = 3-5$), inclusion of the f_{t2} term produces negligible effects. However, if freestream values are chosen near or below the basin of attraction for f_{t2} , then solutions could possibly revert to laminar flow. This boundary for f_{t2} occurs at the critical value $\tilde{\nu}/\nu = \sqrt{\log(c_{t3})/c_{t4}} \approx 0.6$. Rumsey [5] has shown results for cases with freestream values ($\tilde{\nu}/\nu = 1.34$) mildly exceeding this critical value where including the f_{t2} term resulted in boundary layers with laminar-like behavior; these cases also showed pronounced grid dependence. Turbulent behavior was achieved either by eliminating the f_{t2} term ($c_{t3} = 0$) or by choosing a larger freestream value of $\tilde{\nu}/\nu = 3$.

Choosing appropriate freestream values is unfortunately complicated by the fact that some user interfaces do not make it clear whether $\tilde{\nu}$ or ν_t is being set. This creates unnecessary confusion and can lead to users choosing freestream values that are below the critical value when intending to run fully turbulent flow.

2.4 Limiting Maximum Values of $\tilde{\nu}$

There should be no hard-wired limits on the maximum value of $\tilde{\nu}$. Unfortunately, there are a number of flow solvers that do impose such limits, often without notifying the user that the limiter is in effect. This can produce an artificial Reynolds number dependence on solutions and is particularly problematic in full scale aerospace flowfields. Typical limits imposed are $\chi = 10^5$ or 2×10^5 , and these are easily exceeded.

We know of no situations where S-A produces unbounded growth of eddy viscosity (at finite distance), but the model can produce significant levels of eddy viscosity in wakes, jets and separation bubbles. In attached boundary layers, the maximum value across the profile grows with streamwise location x like $\chi_{\max} \sim 0.00059 Re_x^{0.83}$, where Re_x is the Reynolds number based on x . Much larger values are achieved in wakes and jets. For a 2-D plane wake, the asymptotic centerline value is independent of x and depends on

chord-based Reynolds number and drag coefficient as $\chi_{\max} \sim 0.0227Re_c C_d$. For a round jet, the centerline value is also asymptotically independent of x ; it depends on Reynolds number and normalized momentum flux C_M as $\chi_{\max} \sim 0.037Re\sqrt{C_M}$, where both Re and C_M are based on the centerline velocity and jet half-width.

3 Modifications

3.1 Preventing Negative Values of Modified Vorticity \tilde{S}

In physically relevant situations, the modified vorticity \tilde{S} should always be positive with a value that never falls below $0.3S$, where S is the vorticity magnitude. However, discretely this is not always the case. It is possible for \tilde{S} to become zero or negative due to the fact that f_{v2} is itself negative over a range of χ . Negative \tilde{S} in turn disrupts other S-A correlation functions. We present a modified form of \tilde{S} that is identical to the original for $\tilde{S} > 0.3S$, but remains positive for all nonzero S and is C^1 continuous:

$$\bar{S} = \frac{\tilde{v}}{\kappa^2 d^2} f_{v2} \quad (11)$$

$$\tilde{S} = \begin{cases} S + \bar{S} & : \bar{S} \geq -c_{v2}S \\ S + \frac{S(c_{v2}^2 S + c_{v3}\bar{S})}{(c_{v3} - 2c_{v2})S - \bar{S}} & : \bar{S} < -c_{v2}S \end{cases} \quad (12)$$

with $c_{v2} = 0.7$ and $c_{v3} = 0.9$. The modified function is plotted in Fig. 1. The constant c_{v2} controls the patch point; value and derivative with respect to \bar{S} are matched at $\tilde{S} = (1 - c_{v2})S$. The constant c_{v3} controls the asymptote,

$$\tilde{S} \rightarrow (1 - c_{v3})S \quad \text{as} \quad \bar{S}/S \rightarrow -\infty. \quad (13)$$

This modified form of \tilde{S} supersedes the unpublished f_{v3} modification, labeled ‘SA-fv3’ in Ref. [4].

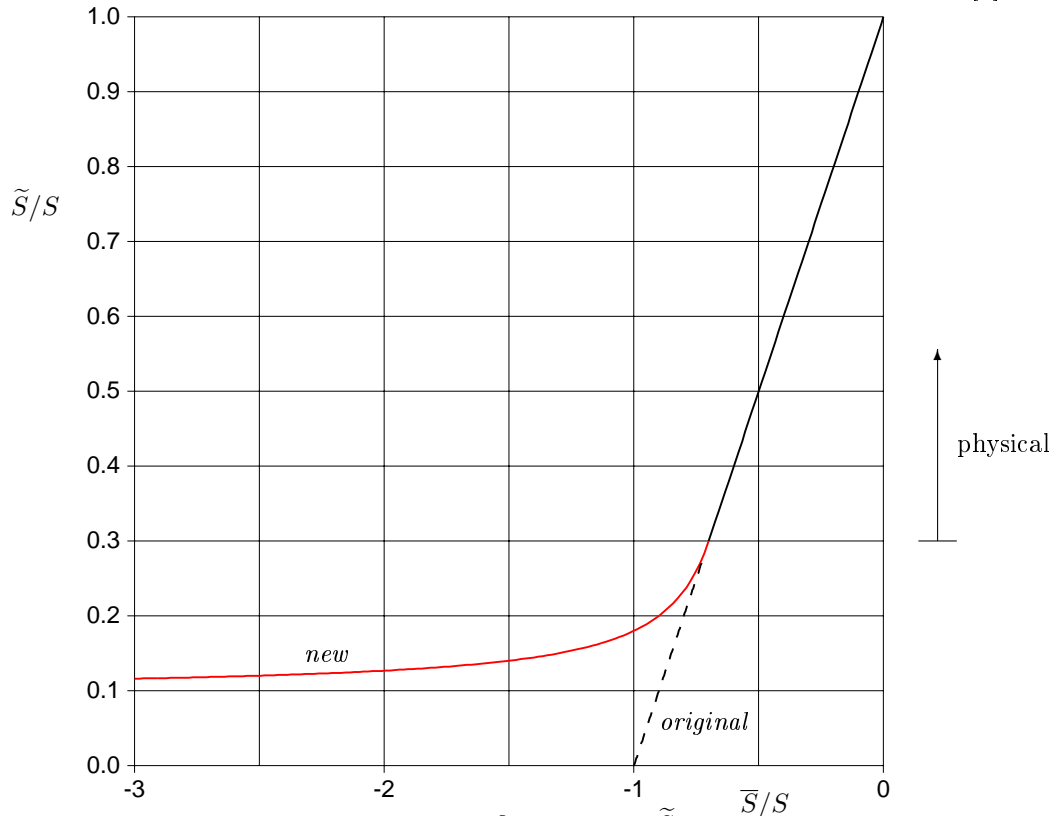


Figure 1: Modified Vorticity \tilde{S}

3.2 Negative S-A Model

The original (positive) S-A model admits only non-negative solutions given non-negative boundary and initial conditions. To see this, consider a smooth solution with local minimum whose value is $\tilde{\nu} = 0$; at this point $\nabla\tilde{\nu} = 0$ and $\nabla^2\tilde{\nu} \geq 0$. Evaluation of S-A at this point produces $\partial\tilde{\nu}/\partial t \geq 0$; thus, the local solution can never decrease below zero. If integration in time produces a steady solution, this argument implies the steady state solution will be everywhere non-negative. This is an analytic argument, and unfortunately, this property is not always obtained discretely. There are situations on coarse grids and transient states where the turbulence solution may become negative. This is often encountered at the edge of boundary layers and wakes where the turbulence solution is characterized by ramp solutions that transition to constant outer/freestream solutions over a short $O((\nu + \tilde{\nu}_\infty)/u)$ region, where u is the entrainment velocity. The rapid transition from large inner to relatively small outer levels can result in undershoots for discrete solutions. These undershoots may cross zero, requiring some action to continue. The common practice in these situations has been to clip updates eliminating negative solution values. However, clipping updates prevents the convergence of discrete PDE residuals and hampers efforts to quantify discrete truncation and solution errors. A number of other approaches appear in the literature; we highlight a few representative examples.

In the original S-A paper [1], positive discrete operators are formulated to ensure that unsteady updates produce non-negative solutions. The most significant limitation of this approach is that the discretization is formally only first order accurate in both space and time due to spacial discretization of the advection terms and the backward Euler time integration. Other limitations include rewriting the diffusion terms ignoring gradients of the molecular viscosity and the requirement for adequate convergence of the resulting implicit system.

Lorin et al [6] use operator splitting and carefully designed discretization to achieve a positive preserving time integration; their spacial and temporal discretizations are second order.

Nguyen et al [7] modify the discretization with artificial dissipation to prevent undershoots in the region of the boundary layer edge. Though promising, the method cannot be shown to produce positive operators and may not prevent negative undershoots in all situations.

Moro et al [8] modify the S-A PDE itself by introducing an alternate working variable that differs from $\tilde{\nu}$ for $\tilde{\nu} < \nu$ and vanishes for $\tilde{\nu}$ sufficiently negative. Our objection here is the modification of S-A for positive $\tilde{\nu}$. In particular, the modified PDE no longer preserves the near-wall behavior of S-A for boundary layers. For tripped cases, the entire laminar and tripped boundary layer regions are influenced by the modifications.

Allmaras [9] developed a negative continuation of the model which required clipping of updates for solution values below a critical negative limit. An early variant of the present formulation was provided to Oliver and appears in his PhD thesis [10].

We formulate a continuation of S-A into the realm of negative $\tilde{\nu}$ solutions to deal with situations of undershoots. Although an analytic continuation of S-A, its primary purpose is to address issues with under-resolved grids and non-physical transient states in discrete settings. The negative S-A model is proposed with the following properties:

- original (positive) S-A is unchanged for $\tilde{\nu} \geq 0$
- negative $\tilde{\nu}$ produces zero eddy viscosity
- functions in the PDE are C^1 continuous with respect to $\tilde{\nu}$ at $\tilde{\nu} = 0$
- negative S-A is energy stable
- the analytic solution is non-negative given non-negative boundary conditions

Consider a negative S-A model of the form,

$$\frac{D\tilde{\nu}}{Dt} = P_n - D_n + \frac{1}{\sigma} \nabla \cdot [(\nu + \tilde{\nu} f_n) \nabla \tilde{\nu}] + \frac{c_{b2}}{\sigma} (\nabla \tilde{\nu})^2 \quad (14)$$

where P_n is production, D_n is wall destruction and $f_n(\chi)$ is a modification to the diffusion coefficient. For C^1 continuity at $\tilde{\nu} = 0$, we require

$$P_n|_0 = D_n|_0 = 0, \quad \left. \frac{\partial P_n}{\partial \tilde{\nu}} \right|_0 = c_{b1}(1 - c_{t3})S, \quad \left. \frac{\partial D_n}{\partial \tilde{\nu}} \right|_0 = 0 \quad (15)$$

$$f_n(0) = 1, \quad \left. \frac{\partial f_n}{\partial \chi} \right|_0 = 0 \quad (16)$$

When $\tilde{\nu}$ is negative, the eddy viscosity is set to zero, and $\tilde{\nu}$ itself becomes a passive scalar. Transport of the energy is given by,

$$\begin{aligned} \frac{D}{Dt} \left(\frac{1}{2} \tilde{\nu}^2 \right) &= \tilde{\nu} \left[P_n - D_n + \frac{1}{\sigma} \nabla \cdot [(\nu + \tilde{\nu} f_n) \nabla \tilde{\nu}] + \frac{c_{b2}}{\sigma} (\nabla \tilde{\nu})^2 \right] \\ &= \tilde{\nu} (P_n - D_n) + \frac{1}{\sigma} \nabla \cdot \left[(\nu + \tilde{\nu} f_n) \nabla \left(\frac{1}{2} \tilde{\nu}^2 \right) \right] - \frac{1}{\sigma} [\nu + \tilde{\nu} (f_n - c_{b2})] (\nabla \tilde{\nu})^2 \end{aligned} \quad (17)$$

The usual requirements for energy stability then give the constraints,

$$P_n - D_n \geq 0, \quad 1 + \chi (f_n - c_{b2}) \geq 0. \quad (18)$$

These will ensure that integrated energy decreases in time, forcing negative transients back towards zero. We can go further and formulate the PDE to eliminate the existence of negative steady state solutions in the analytic limit. This will ensure for sufficiently refined grids that the solution will be everywhere non-negative. To achieve this goal, we consider requirements necessary to prevent a smooth negative minimum to persist in the steady state. At the point in question, $\nabla \tilde{\nu} = 0$ and $\nabla^2 \tilde{\nu} \geq 0$. The resulting steady PDE is,

$$P_n - D_n + \frac{1}{\sigma} (\nu + \tilde{\nu} f_n) \nabla^2 \tilde{\nu} = 0 \quad (19)$$

If individual terms are all non-negative, then the steady PDE cannot be satisfied at this point, precluding the existence of smooth negative minimums in the solution. The resulting requirements are,

$$P_n - D_n \geq 0, \quad 1 + \chi f_n \geq 0. \quad (20)$$

The diffusion coefficient requirement is more restrictive than that for energy stability.

The above requirements are not mutually exclusive and we have significant flexibility to define a negative extension of S-A. The final requirements are C^1 continuity (Eq. 15) and prevention of negative minimums in the steady solution (Eq. 20). We strive to mitigate nonlinearity. If the diffusion coefficient mimics the positive model behavior for large $|\tilde{\nu}|$, then f_n should asymptote to -1 . Maximizing the region over which the diffusion coefficient turns from $\nu + \tilde{\nu}$ for positive to $\nu + |\tilde{\nu}|$ for large negative, we arrive at,

$$f_n = \frac{c_{n1} + \chi^3}{c_{n1} - \chi^3} \quad (21)$$

with $c_{n1} = 16$. The diffusion coefficient $\nu + \tilde{\nu} f_n$ is everywhere positive as shown in Fig. 2. A negative diffusion coefficient first occurs with $c_{n1} \approx 16.46$, which limits the magnitude of this parameter.

The inclusion of f_{t2} in positive S-A is important in that the derivative (Eq. 15) at $\tilde{\nu} = 0$ is negative since $c_{t3} > 1$. This means that it is possible to define P_n positive for all negative $\tilde{\nu}$, as well as matching the derivative at zero. Although Eq. 20 places a constraint on the combined production and destruction terms, we define individually production to be positive and destruction to be negative,

$$P_n = c_{b1} (1 - c_{t3}) S \tilde{\nu}, \quad D_n = -c_{w1} \left[\frac{\tilde{\nu}}{d} \right]^2 \quad (22)$$

Note that P_n is defined in terms of vorticity S rather than modified vorticity \tilde{S} as in the positive model. Also note the sign change on D_n compared to the positive model. Figure 3 shows a plot of production for a fixed location in space; the normalization $d\sqrt{S}/\tilde{\nu}$ is similar to wall units but uses the local vorticity instead of the wall value. Inclusion of f_{t2} forces the production negative for small positive values of $\tilde{\nu}$ and gives the negative derivative at zero in Eq. 15. The negative production term P_n is linear with this same derivative value. In contrast, removal of the f_{t2} term from S-A results in a production term that is roughly linear for positive $\tilde{\nu}$ at this value of $d\sqrt{S}/\tilde{\nu}$. This causes a problem for defining a negative continuation of

the production term. Either C^1 continuity must be given up or $P_n < 0$ must be allowed for some region of negative χ , potentially violating Eqs. 18 and 20.

The negative model consisting of Eqs. 14, 21 and 22 should be applicable to a wide range of discretization methods, including higher order methods. It is expected that no additional limiting or artificial dissipation should be necessary in the vicinity of negative undershoots. On coarse grids, small regions of negative $\tilde{\nu}$ solution states will likely occur for both steady and unsteady solutions near the edges of boundary layers and wakes. As the grid is refined, these regions should diminish both in magnitude and physical extent, and they should disappear altogether with sufficiently fine grid.

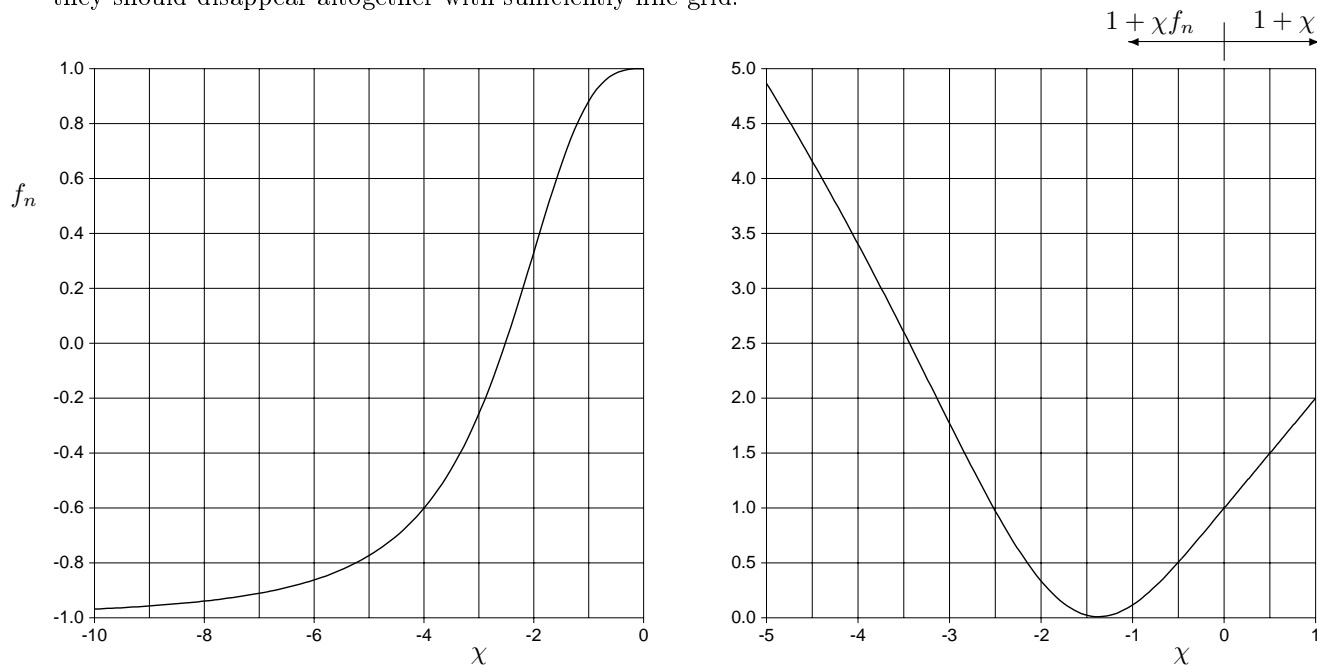


Figure 2: Diffusion coefficient for negative model

3.3 Inviscid Wall Boundary Condition

The original S-A references prescribed a zero Neumann condition, $\partial\tilde{\nu}/\partial n = 0$, for inviscid walls. We now propose treating inviscid walls, also referred to as slip walls, using a zero Dirichlet boundary condition, $\tilde{\nu} = 0$, and specify that the wall should be included in the computation of the distance function (i.e. $d = 0$ at the inviscid wall). The rationale for this change is re-examination of the blocking effect of inviscid walls on the development of Reynolds stresses. We also draw a distinction between turbulent boundary conditions for (straight) inviscid walls and planes of symmetry; these have traditionally been considered synonymous in CFD.

As an example flow, consider the plane wake of a symmetric body. Boundary conditions are symmetric and the resulting mean flow is symmetric about the centerline ($y = 0$). The instantaneous velocity field, however, may not always be symmetric, but any asymmetries must vanish upon averaging. In particular, the instantaneous normal velocity v' may be nonzero on the centerline at any given time, but averaging gives zero mean. The resulting Reynolds shear stress $\overline{u'v'}$ has been experimentally shown to be nearly proportional to the mean strain $\partial u/\partial y$, giving constant eddy viscosity as a good approximation. For S-A the appropriate boundary condition for this flow is zero Neumann, $\partial\tilde{\nu}/\partial n = 0$, at the centerline, and the distribution of $\tilde{\nu}$ across the wake is bell shaped with its maximum at the centerline.

Now consider the same flowfield with an inviscid splitter plate along the centerline. Here the instantaneous normal velocity is always zero on the centerline, and there is no transfer of momentum across the splitter plate. These differences must be reflected in the distribution of velocity and Reynolds shear stress across the wake. In particular, $\overline{u'v'}$ must grow more slowly away from the centerline than it would without the

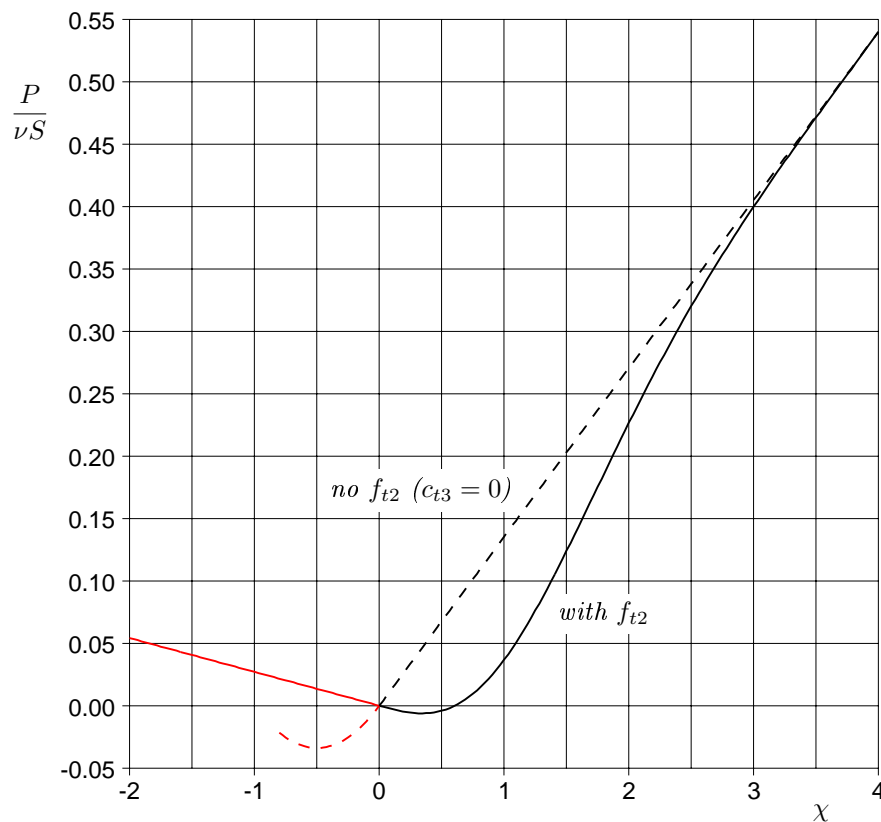


Figure 3: Production for negative model; $d\sqrt{S/\nu} = 100$

splitter plate. This blocking effect of the splitter plate should be reflected in boundary conditions imposed on the turbulence solution. We propose for this flow that $\tilde{\nu} = 0$ at the centerline and the associated distance function is $d = |y|$.

This change in turbulence boundary condition for inviscid walls is nontrivial. It means that the S-A solution will be anisotropic in the vicinity of the wall particularly for high Reynolds number flows. For fully turbulent flows, $\tilde{\nu}$ will fall from ambient values (e.g. freestream) to zero over a small lateral distance. Comparable streamwise variations will occur over a much larger distance. The scales involved should be similar to laminar boundary layers. In contrast, the velocity field will remain largely isotropic near the wall with only minor effects of molecular and eddy viscosity due to the small strains involved.

4 Analytic Solution

4.1 Analytic Solution for Law of the Wall Velocity

S-A is formulated to permit the following simple solution for law of the wall,

$$\tilde{\nu} = \kappa u_\tau y, \quad \tilde{S} = \frac{u_\tau}{\kappa y}, \quad (23)$$

where u_τ is the shear stress velocity, y is distance from the wall and $\kappa = 0.41$ is von Karman's constant. Integrating this solution to give an explicit expression for velocity has proven difficult due to the complexity of the eddy viscosity correlation function f_{v1} , which also enters into the definition of \tilde{S} . We present a new analytic solution for velocity $u(y)$ that is consistent with S-A in the law of the wall region. The following analysis is also presented in an appendix attributed to the first author in Berger and Aftosmis [11].

We make the usual assumptions for law of the wall analysis: incompressible, zero pressure gradient, constant outer (edge) velocity, advection terms are negligible and $\partial/\partial x \ll \partial/\partial y$, where x is streamwise and

y normal to the wall. With these assumptions, $u = u(y)$ and $\tilde{\nu} = \tilde{\nu}(y)$, and the x -momentum equation reduces to a statement of constant total shear stress,

$$\frac{d}{dy} \left[(\nu + \nu_t) \frac{du}{dy} \right] = 0, \quad \rightarrow \quad (\nu + \nu_t) \frac{du}{dy} = \text{const} = u_\tau^2, \quad (24)$$

where u_τ is the wall shear stress velocity. With these same assumptions, S-A reduces to,

$$\frac{1}{\sigma} \frac{d}{dy} \left[(\nu + \tilde{\nu}) \frac{d\tilde{\nu}}{dy} \right] + \frac{c_{b2}}{\sigma} \left[\frac{d\tilde{\nu}}{dy} \right]^2 + c_{b1} (1 - f_{t2}) \tilde{S} \tilde{\nu} - \left(c_{w1} f_w - \frac{c_{b1}}{\kappa^2} f_{t2} \right) \left[\frac{\tilde{\nu}}{y} \right]^2 = 0, \quad (25)$$

where

$$\nu_t = \tilde{\nu} f_{v1}, \quad f_{v1} = \frac{\chi^3}{\chi^3 + c_{v1}^3}, \quad \chi \equiv \frac{\tilde{\nu}}{\nu}, \quad (26)$$

and

$$\tilde{S} = \frac{du}{dy} + \frac{\tilde{\nu}}{\kappa^2 y^2} f_{v2}, \quad f_{v2} = 1 - \frac{\chi}{1 + \chi f_{v1}}, \quad f_{t2} = c_{t3} \exp(-c_{t4} \chi^2). \quad (27)$$

By construction, these equations have the simple solution Eq. 23. Transforming to wall units, $y^+ \equiv y u_\tau / \nu$ and $u^+ \equiv u / u_\tau$, this solution becomes,

$$\chi = \kappa y^+, \quad \tilde{S}^+ = \frac{\nu}{u_\tau^2} \tilde{S} = \frac{1}{\kappa y^+}. \quad (28)$$

This solution is the extension of well known log-law behavior to the entire inner layer from the wall through the viscous sublayer and into the log-law region. In the log layer, Reynolds' stresses dominate molecular stresses. With the introduction of the Boussinesq approximation and the log-law velocity distribution, both velocity gradient and eddy viscosity can be determined,

$$\frac{\nu_t}{\nu} = \kappa y^+, \quad \frac{du^+}{dy^+} = \frac{1}{\kappa y^+}, \quad y^+ \gg 1. \quad (29)$$

In developing the near-wall or viscous sublayer components of S-A, this simple behavior was retained for the new solution variable $\tilde{\nu}$ and the modified vorticity \tilde{S} by introducing the eddy viscosity correlation function f_{v1} , the definition of modified vorticity (via f_{v2}) and the re-definition of r (Eq. 5). The function f_{v1} was taken from Mellor and Herring [12]. Note that the presence of the laminar suppression term, f_{t2} , in S-A is passive with respect to the simple solution; contributions from production and wall destruction cancel in Eq. 25.

Substituting the simple solution (Eq. 28) into either x -momentum or the definition for \tilde{S} then gives,

$$\frac{du^+}{dy^+} = \frac{c_{v1}^3 + (\kappa y^+)^3}{c_{v1}^3 + (\kappa y^+)^3 (1 + \kappa y^+)} \quad (30)$$

This equation can be integrated (via Mathematica[13]) and the constant of integration determined from the no-slip boundary condition $u(0) = 0$. Using complex arithmetic, the solution is,

$$u^+(y^+) = \sum_{i=1}^4 \frac{c_{v1}^3 + z_i^3}{\kappa z_i^2 (3 + 4z_i)} \left[\log(\kappa y^+ - z_i) - \log(-z_i) \right], \quad (31)$$

where z_i are the four solutions to the quartic equation,

$$c_{v1}^3 + z_i^3 + z_i^4 = 0 \quad (32)$$

The solution can be simplified and rewritten using real arithmetic,

$$u^+(y^+) = \bar{B} + c_1 \log((y^+ + a_1)^2 + b_1^2) - c_2 \log((y^+ + a_2)^2 + b_2^2) - c_3 \text{ArcTan}[y^+ + a_1, b_1] - c_4 \text{ArcTan}[y^+ + a_2, b_2], \quad (33)$$

where $\text{ArcTan}[x, y]$ is the Mathematica function equivalent to the Fortran function $\text{atan2}(y, x)$. For the values of $\kappa = 0.41$ and $c_{v1} = 7.1$, the constants are given by,

$$\begin{aligned} \bar{B} &= 5.0333908790505579 \\ a_1 &= 8.148221580024245 & b_1 &= 7.4600876082527945 \\ a_2 &= -6.9287093849022945 & b_2 &= 7.468145790401841 \\ c_1 &= 2.5496773539754747 & c_2 &= 1.3301651588535228 \\ c_3 &= 3.599459109332379 & c_4 &= 3.6397531868684494 \end{aligned}$$

Analysis of this solution for large y^+ reveals that S-A asymptotically produces a log-law with a shifted origin compared to the conventional formulas,

$$u^+ \sim \frac{1}{\kappa} \log(y^+ + 1/\kappa) + \bar{B}, \quad \frac{du^+}{dy^+} \sim \frac{1}{\kappa y^+ + 1}, \quad \text{as } y^+ \rightarrow \infty. \quad (34)$$

The shift in the asymptotic gradient can also be derived from Eq. 30. The origin shift is minor, but is easily noticeable in law of the wall velocity plots. The shift has no special meaning, but is a detail of the model's behavior.

Figure 4 shows the law of the wall velocity profile for S-A (Eq. 33) compared to its asymptotic form (Eq. 34) and to Spalding's composite formula,

$$y^+ = u^+ + \exp(-\kappa B) \left[\exp(\kappa u^+) - 1 - \kappa u^+ - \frac{1}{2}(\kappa u^+)^2 - \frac{1}{6}(\kappa u^+)^3 \right]. \quad (35)$$

Here the values of $\kappa = 0.41$ and $B = 5$ have been plotted; this value of B is consistent with the calibration of S-A (and in particular $c_{v1} = 7.1$).

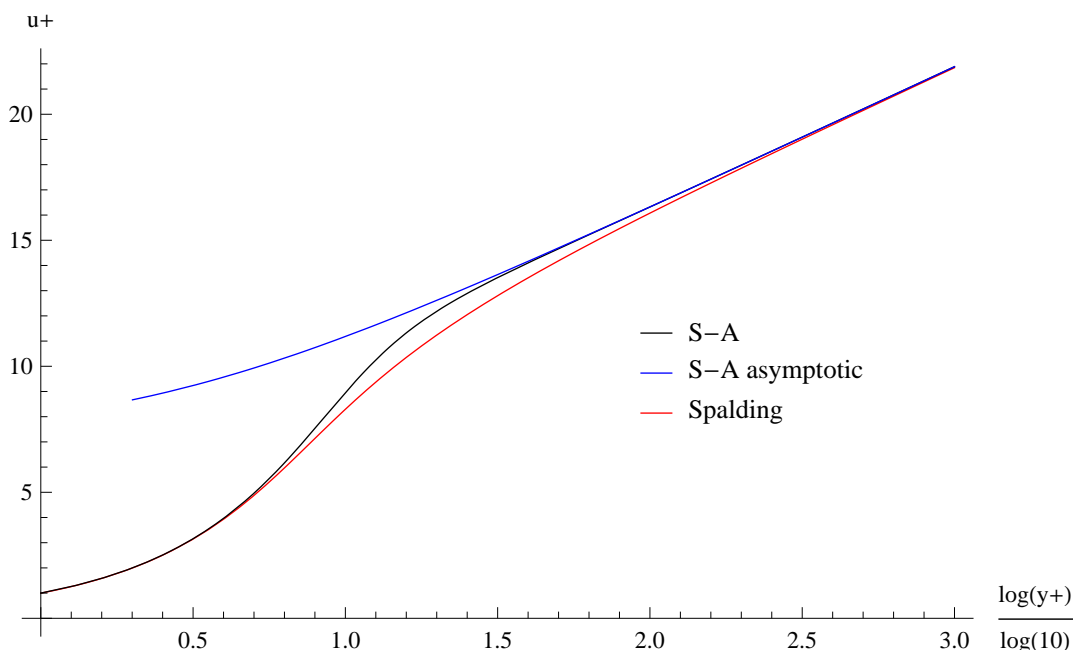


Figure 4: Law of the Wall velocity profile

The analytic solution, Eq. 33, can be used to construct wall functions for flow solvers. It offers a simplified implementation over the Spalding formula due to the fact that the velocity is an explicit function.

Wall function implementations that utilize Spalding require localized Newton solves because of its implicit form. For flow solvers using S-A, wall functions based on Eq. 33 provide the added benefit of consistency with the model.

The analytic solution can also be used for code validation. Near-wall solutions for Couette flow at high Reynolds numbers should be very close to Eq. 33. The analytic solution could also be used for comparison in test cases specifically set up to reproduce the viscous sublayer and log layer behaviors of S-A. This could be achieved by imposing Eqs. 23 and 34 as outer boundary conditions.

Acknowledgements

The analytic solution was discovered while the first author was under contract with the NASA Ames Educational Associates Program. Dr. W. K. Anderson implemented the negative S-A model and provided feedback.

References

- [1] Spalart, P. R., and Allmaras, S. R., “A One-Equation Turbulence Model for Aerodynamic Flows”, AIAA-92-0439, January 1992.
- [2] Spalart, P. R., and Allmaras, S. R., “A One-Equation Turbulence Model for Aerodynamic Flows”, *La Recherche Aéronautique*, no 1, 1994, pp. 5-21.
- [3] Rumsey, C. L., and Spalart P. R., “Turbulence Model Behavior in Low Reynolds Number Regions of Aerodynamic Flowfields”, *AIAA Journal*, vol 47, no 4, pp. 982-993, 2009. Technology, June 2008.
- [4] Rumsey, C. L., Smith, B. R., Huang, G. P., “Description of a Website Resource for Turbulence Model Verification and Validation”, AIAA-2010-4742, 40th AIAA Fluid Dynamics Conference, June 2010. See also <http://turbmodels.larc.nasa.gov>
- [5] Rumsey, C. L., ‘Apparent Transition Behavior of Widely Used Turbulence Models’, *International Journal of Heat and Fluid Flow*, vol 28, no 6, pp. 1460-1471, 2007.
- [6] Lorin, E., Benhajali, A., Soulaïmani, A., “A Positivity Preserving Finite Element-Finite Volume Solver for The Spalart-Allmaras Turbulence Model”, *Computer Methods in Applied Mechanics and Engineering*, vol 196, issue 17-20, pp. 2097-2116, 2007.
- [7] Nguyen, N. C., Persson, P.-O., and Peraire, J., “RANS Solutions Using High Order Discontinuous Galerkin Methods”, AIAA-2007-914, January 2007.
- [8] Moro, D., Nguyen, N. C., Peraire, J., “Navier-Stokes Solution Using Hybridizable Discontinuous Galerkin Methods”, AIAA-2011-3407, June 2011.
- [9] Allmaras, S. R., “Multigrid for the 2-D Compressible Navier-Stokes Equations”, AIAA-99-3336, July 1999.
- [10] Oliver, T. A., “A Higher-Order, Adaptive, Discontinuous Galerkin Finite Element Method for the Reynolds-Averaged Navier-Stokes Equations”, Ph.D. thesis, Department of Aeronautics and Astronautics, Massachusetts Institute of Technology, June 2008.
- [11] Berger, M., Aftosmis, M., “Progress Towards a Cartesian Cut-Cell Method for Viscous Compressible Flow”, AIAA-2012-1301, January 2012.
- [12] Mellor, G. L., Herring, H. J., “Two Methods of Calculating Turbulent Boundary Layer Behavior Based on Numerical Solution of the Equations of Motion”, Proc. Conf. Turb. Boundary Layer Pred., Stanford, 1968.
- [13] *Mathematica*, Version 8, Wolfram Research, Inc., Champaign, IL (2011).